Journal of Biomolecular NMR, **20:** 83–88, 2001.
KLUWER/ESCOM

Domain orientation in β-cyclodextrin-loaded maltose binding protein: Diffusion anisotropy measurements confirm the results of a dipolar coupling study

Peter M. Hwang, Nikolai R. Skrynnikov & Lewis E. Kay
Protein Engineering Network Center of Excellence and Departments of Medical Genetics, Biochemistry and Chemistry, University of Toronto, Toronto, ON, Canada M5S 1A8

Received 13 February 2001; Accepted 27 March 2001

Key words: diffusion tensor, domain orientation, maltose binding protein, ^{15}N relaxation

Abstract

Maltose binding protein (MBP) is a 370-residue two-domain molecule involved in bacterial chemotaxis and sugar uptake. Rotational diffusion tensors were calculated for a complex between MBP and β-cyclodextrin using backbone ^{15}N T_1 and $T_{1\rho}$ relaxation times and steady state ^{1}H-^{15}N NOE values. The tensors obtained for each of the two domains in the protein were subsequently used to determine the relative domain orientation in the molecule. The average domain orientation determined using this approach agrees well with results from dipolar coupling data, but differs significantly from the domain orientation deduced from X-ray studies of the complex.

Considerable conformational freedom can exist between the individual domains of a multi-domain protein (Alber et al., 1983). In many cases this flexibility is essential to proper function, including optimizing substrate sequestration and release during enzyme catalysis and controlling ligand binding (Karplus and McCammon, 1983; Fersht, 1985). Changes in domain orientation in response to biological stimuli provide a mechanism for regulation and signal transduction (Pawson, 1995). To date much of the information available about how multi-domain proteins change in conformation as a function of ligand binding or covalent modification, such as phosphorylation, derives from X-ray crystallography. However, in some cases inter-domain conformations deduced by X-ray methods are biased because of crystal packing interactions (Faber and Matthews, 1990; Zhang et al., 1995) and the need for alternative approaches is apparent.

Recent developments in NMR spectroscopy have facilitated structural studies of multi-domain systems (Prestegard, 1998; Wider and Wüthrich, 1999). In particular, weak magnetic alignment achieved with phage (Clore et al., 1998; Hansen et al., 1998) or bicelle (Tjandra and Bax, 1997) media allows measurement of residual dipolar couplings in biomolecules. These couplings, in turn, can be analyzed to determine molecular alignment tensors for individual protein domains and relative domain orientations can be subsequently established by examination of the principal axes of the tensors from these domains (Fischer et al., 1999; Skrynnikov et al., 2000). An alternate method that does not require aligning media involves the measurement of heteronuclear relaxation rates to determine rotational diffusion tensors (Tjandra et al., 1995) for each domain (Brüschweiler et al., 1995; Tjandra et al., 1997; Fushman et al., 1999). The principal axes of these tensors can be aligned to obtain relative domain orientations in a manner analogous to the situation with dipolar coupling data.

E. coli maltose binding protein, MBP, is a 370-residue periplasmic protein with two domains of roughly equal size. Crystal structures of the apo (Sharff et al., 1992) and holo (Spurlino et al., 1991) forms suggest that the two domains close by roughly 35° upon maltose binding. It is believed that this conformational change is important for recognition by membrane bound receptors, a first step in maltose uptake by active transport and in chemotaxis

(Mowbray and Sandgren, 1998). In contrast to the crystal structures of the maltose-, maltotriose- and maltotetraose-bound states of MBP, the X-ray structure of the β-cyclodextrin bound form is very similar to the open apo form (Sharff et al., 1993). However, a recent residual dipolar coupling-based determination of domain orientation in the protein suggested that the solution form of the MBP–β-cyclodextrin complex is significantly more closed (∼11°) than what had been previously reported from an analysis of the X-ray structure (Skrynnikov et al., 2000).

Although it has been shown in a number of cases that alignment induced by weak interactions of single-domain proteins with the alignment media does not affect tertiary structure (Koenig et al., 1999; Ojennus et al., 1999; Sass et al., 1999), the energy barriers separating different domain orientations in multi-domain proteins are often small, and the influence of media on the domain orientations that are determined from dipolar couplings is therefore a potential concern. In order to establish that differences in solution and crystal states of the β-cyclodextrin-loaded MBP complex (Skrynnikov et al., 2000) are not the result of interactions between the protein and the phage used for alignment, we have calculated relative domain orientations in the isotropic phase using ^{15}N-relaxation-based rotational diffusion measurements, as described below. The relative domain orientation obtained using this approach is consistent with the results derived from the dipolar coupling study.

^{15}N T_1, $T_{1\rho}$ and steady state ^{1}H-^{15}N NOEs were recorded on the MBP–β-cyclodextrin complex, with a number of representative T_1 and $T_{1\rho}$ decay curves illustrated in Figure 1. All data sets were obtained using TROSY-based pulse schemes (Pervushin et al., 1997) to maximize spectral resolution and hence increase the number of residues available for analysis. Relaxation data from 95 residues in the N-domain (residues 6–109 and residues 264–309) and 114 residues in the C-domain (114–258, 316–370) were extracted. Residues for which steady state ^{1}H-^{15}N NOE values were less than 0.65 were eliminated from further analysis (Tjandra et al., 1995) and rotational diffusion tensors were calculated separately for each of the domains using T_1/T_2 ratios of individual residues, as described by Tjandra and Bax (1995) and Lee et al. (1997). The fits, described below, were significantly improved when an axially symmetric rotational diffusion model was used in place of an isotropic one, but only a very modest improvement was obtained by switching to the fully anisotropic model (N-domain, $p = 0.07$; C-domain, p

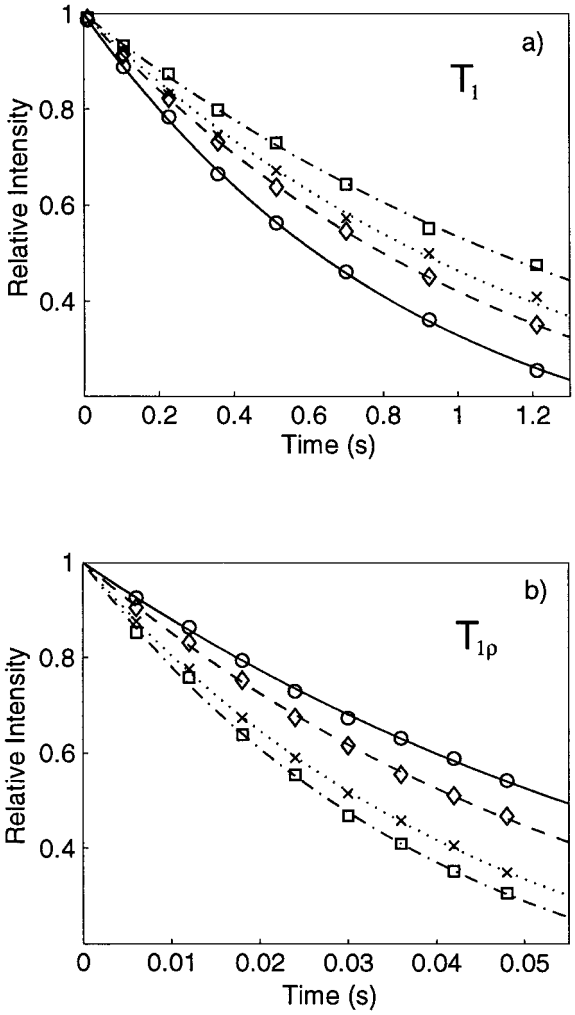

Figure 1. (a) ^{15}N T_1 and (b) ^{15}N $T_{1\rho}$ relaxation curves for selected MBP residues: ◯, Gly56; □, Lys119; ×, Ser211; ◊, Lys370. The sample used in the present study comprised 1.4 mM ^{15}N,^{13}C,^{2}H-labeled protein, with protonation at the methyl groups of Val, Leu, and Ile (δ1 only), 2 mM β-cyclodextrin, 20 mM phosphate (pH 7.2), 3 mM NaN_3, 100 μM EDTA, 10% ^2H_2O. The protein was expressed and purified as described previously (Goto et al., 1999). Spectra were recorded at 37 °C on a 600 MHz Varian Inova spectrometer. T_1, $T_{1\rho}$ and steady state ^{1}H-^{15}N NOE values were recorded according to previously published pulse sequences (Farrow et al., 1994), with modifications to make use of the TROSY principle (Pervushin et al., 1997). Delay times for the T_1 experiments were 10, 106, 227, 358, 515, 702, 924, and 1212 ms and for the $T_{1\rho}$ experiments, 6, 12, 18, 24, 30, 36, 42, and 48 ms. A 1.68 kHz ^{15}N spin-lock field was applied during the $T_{1\rho}$ relaxation delay. Steady state ^{1}H-^{15}N NOEs were obtained by recording one spectrum with a 10 s recycle delay followed by 5 s saturation and another spectrum with no saturation and a 15 s recycle delay. Relaxation rates and errors were obtained as described previously (Farrow et al., 1994). $T_{1\rho}$ values were converted to T_2 values according to $1/T_{1\rho} = \cos^2\theta/T_2 + \sin^2\theta/T_1$, where $\theta = \tan^{-1}(\Omega_N/\gamma_N B_1)$, Ω_N is the resonance offset and $\gamma_N B_1$ is the spin-lock field strength (Peng and Wagner, 1992).

= 0.60, where p is the probability that the improvement in fit using the fully anisotropic model relative to the axially symmetric one is due to chance). Hence all subsequent diffusion tensor calculations assumed an axially symmetric model. Of interest, in the case where a fully anisotropic model was employed D_Y/D_X ratios of 1.08 and 1.04 were obtained for the N- and C-domains, respectively, and the D_i values (D_i is the $i = \{x, y, z\}$ component of the diffusion tensor) between domains were very similar. This implies that both domains exhibit similar rotational dynamics.

An axially symmetric diffusion tensor is described in terms of two polar angles, θ and ϕ, indicating the orientation of the unique axis of the diffusion frame with respect to some molecular frame, as well as by diffusion coefficients, $D_\parallel$ and $D_\perp$, where $D_\parallel = D_Z$ and $D_\perp = D_X = D_Y$ (Woessner, 1962). As described in detail in the literature, the diffusion tensor parameters can be extracted by minimizing the difference between experimentally derived relaxation rates and those predicted on the basis of a model structure, Equations 1 and 2 below (Tjandra et al., 1995; Lee et al., 1997; Tsan et al., 2000). We have written a program that calculates relaxation rates of ^{15}N spins in MBP incorporating the dominant contributions from ^{15}N-^{1}H dipolar and ^{15}N CSA-induced relaxation interactions (Kay et al., 1989) as well as the ^{15}N-^{13}CO and ^{15}N-$^{13}C_\alpha$ dipolar interactions that are present in a ^{13}C-labeled sample. For the ^{15}N-^{1}H dipolar interaction a bond length of 1.02 Å was employed and an axially symmetric ^{15}N chemical shift tensor with an anisotropy of -172 ppm was assumed (Ishima and Torchia, 2000), with the unique axis of the tensor tilted 20° towards the carbonyl bond (Cornilescu and Bax, 2000). Spectral densities were calculated according to Equation 6 of Tjandra and Bax (1995), which includes anisotropic diffusion and rapid internal dynamics. Although the assumption of separability of anisotropic overall motion and internal dynamics inherent in this model is not completely rigorous, it is reasonable in cases where the timescales of the two motions are very different (Lipari and Szabo, 1982a, b).

In order to ascertain that the diffusion tensor parameters obtained were not sensitive to the details of the fitting procedure we have used three different approaches in our calculations. In the first approach T_1/T_2 ratios are predicted for every residue in a protein domain, $(T_1/T_2)_{pred}$, using an X-ray structure of MBP and compared to experimental T_1/T_2 ratios, $(T_1/T_2)_{expt}$, according to the error function

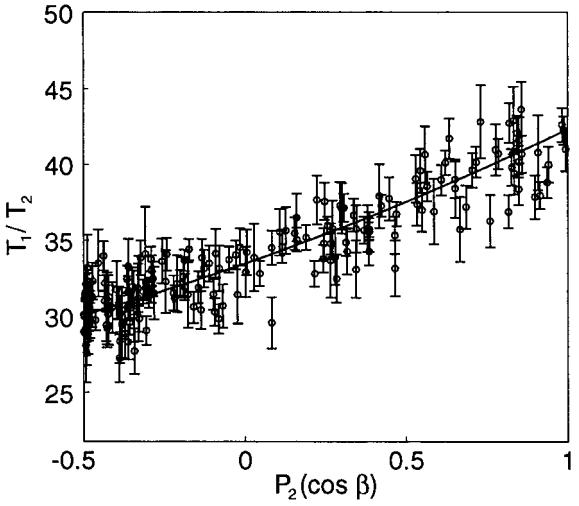

Figure 2. Predicted (solid line) and experimentally determined (data points) T_1/T_2 ratios plotted as a function of $P_2(\cos\beta)$, where β is the angle that the NH bond makes with the unique axis of the diffusion tensor. NH bond vectors from both domains are included in the figure. Diffusion tensor parameters were calculated separately for each domain using method 1 (see text) and the crystal structure 1OMP (Sharff et al., 1992b). Errors in T_1/T_2 ratios are indicated by vertical bars. Outliers (see text) have been removed. $P_2(x)$ is the second order Legendre polynomial, $P_2(x) = 0.5(3x^2 - 1)$. Note that the calculation assumes a 20° angle between the ^{15}N CSA long axis and the NH bond, as discussed in the text.

$$|\chi| = \sum_i |\chi_i| = \sum_i \left| \frac{(T_1/T_2)_{expt,i} - (T_1/T_2)_{pred,i}}{\sigma_{T1/T2,i}} \right| \quad (1)$$

where $\sigma_{T1/T2}$ is the calculated experimental error in the T_1/T_2 ratio and the sum extends over all the residues in the domain for which data are obtained (Tjandra et al., 1995). The four fitting parameters $D_\parallel$, $D_\perp$, θ and ϕ are obtained from minimization of $|\chi|$. It is known that these values can be sensitive to the presence of outliers, i.e., data points affected by complex local dynamics (Tjandra et al., 1995). With this in mind, after the first round of minimization, residues for which $|\chi_i| > 4$ are removed and the process is repeated until no additional $|\chi_i|$ values of this magnitude are obtained. Figure 2 illustrates the correlation between $(T_1/T_2)_{expt}$ and the orientation of N-H bond vectors relative to the unique axis of the diffusion tensor determined from the 1OMP crystal structure (Sharff et al., 1992b). The correlation includes results from both domains which were fitted separately.

In the second approach, the diffusion tensor parameters are optimized using T_1/T_2 ratios as in method 1, beginning with all residues for which data

are available and for which ^{1}H-^{15}N steady state NOE values are greater than 0.65. After each iteration, values for the square of the order parameter and effective correlation time for fast timescale dynamics, S^2 and τ_e (Lipari and Szabo, 1982a, b), were calculated for each residue by performing a minimization of δ_i^2:

$$\delta_i^2 = \frac{(T_{1,i}^{expt} - T_{1,i}^{pred})^2}{\sigma_{T1,i}^2} + \frac{(T_{2,i}^{expt} - T_{2,i}^{pred})^2}{\sigma_{T2,i}^2} + \frac{(NOE_i^{expt} - NOE_i^{pred})^2}{\sigma_{NOE,i}^2}. \quad (2)$$

Any residue for which $\delta_i^2 > 18.75$ was removed and the diffusion tensor was recalculated as before. Thus, this approach involves a nested optimization, with an outer loop used to determine diffusion parameters and an inner loop to identify the residues with inconsistent T_1, T_2 and NOE values which are excluded from subsequent analysis. A third method, similar to the second approach, was also employed in which the average values of S^2 (0.87) and τ_e (11.8 ps) obtained from method 2 were used in the calculation of optimal diffusion parameters (in contrast to $S^2 = 1$ that was employed at this stage in method 2). Diffusion tensor values were subsequently generated and outliers removed as with method 2. Note that all methods described above automatically reject data points with substantial contributions from chemical exchange to $1/T_2$ rates. We have also carried out additional experiments at 500 MHz to establish that there are no exchange contributions in excess of 4 s^{-1}.

Approximately 5% of the data points were removed in any given method using the criteria described above. In most cases a single iteration was sufficient to remove outliers; in several cases as many as three iterations were necessary. We have verified that further removal of data points had essentially no effect on the determined diffusion parameters (i.e., that the procedure for removing outliers leads to a stable solution).

In order to estimate the influence of slight differences in input X-ray structures (structural noise) on the extracted diffusion tensor parameters, each of the three methods was applied to four different X-ray crystal structures of MBP (Table 1). For each starting input X-ray structure ('parent' structure) diffusion tensor parameters were obtained for both N- and C-domains independently. Subsequently, the unique axes of the diffusion frames from the two domains were aligned, in the process reorienting the N-domain of the protein with respect to the C-domain to generate an NMR-derived 'daughter' structure.

In order to characterize daughter structures generated using this approach, all structures are first placed in the same coordinate frame by superposition of their C-terminal domains with the corresponding domain of the X-ray structure, 1OMP (Sharff et al., 1992a). Subsequently, each 'daughter' conformation can be described in terms of closure, bend and twist relative to the reference structure 1OMP as discussed previously by Skrynnikov et al. (2000) and illustrated in Figure 3. In this manner, we obtained a range of domain closure angles (relative to the apo form, 1OMP) varying from 10 to 19°, Table 1. The average values of closure and bend, 15° and 0°, respectively, calculated from diffusion anisotropy data agree well with the corresponding averages (14° closure and −2° bend) obtained from dipolar coupling measurements (Skrynnikov et al., 2000). This provides strong evidence that use of aligning media (phage) in the dipolar coupling study did not alter the inter-domain conformation of MBP and that there are significant differences between the X-ray structure of the protein and the conformation observed in solution, as reported previously (Skrynnikov et al., 2000).

As a final note it is important to emphasize that the diffusion tensors obtained in the present study are axially symmetric. As such there is an extra degree of freedom (rotation about the symmetry axis of the diffusion tensor) for which no information is available from the present set of measurements. Thus, once the unique axes of the diffusion tensors for the two domains are aligned it is possible to rotate one domain relative to the other about the resulting unique axis without affecting the level of agreement between measured and calculated relaxation parameters. Since this axis is nearly collinear with the twist axis (between 4°–9°, depending on the input X-ray structure), the closure and bend angles are only minimally affected by such rotations. Assuming a (large and likely unphysical) rotation of 20° about this axis, closure and bend angles are changed by no more than 2° and 4°, respectively. Thus, in the present study closure and bend angles are relatively well defined, but twist is not.

In summary, the inter-domain conformation of β-cyclodextrin-loaded MBP has been determined using backbone ^{15}N spin relaxation methods. The domain orientation obtained from the present approach agrees well with that generated from a dipolar coupling based methodology, but is significantly different (12° closure) from what has been reported in an X-ray study

Table 1. Average diffusion tensor parameters of β-cyclodextrin-loaded MBP. Global correlation time, $\tau_{C,eff}$: 18.6 ± 0.4 ns[a]; diffusion anisotropy, $D_{\parallel}/D_{\perp}$: 1.39 ± 0.05

Starting crystal structure[b]	Closure, twist, and bend relative to 1OMP from ^{15}N relaxation data[c]	Closure, twist, and bend relative to 1OMP from dipolar coupling data (Skrynnikov et al., 2000)
1OMP	17°, 0°, 0°	13°, 0°, −4°
1DMB	10°, 0°, −3°	15°, 4°, −4°
1ANF	19°, −1°, 3°	15°, 0°, 0°
4MBP	14°, 0°, 2°	13°, 4°, 0°

[a] $\tau_{C,eff} = 1/(4D_{\perp} + 2D_{\parallel})$. Diffusion tensor parameters were calculated by three different methods (see text) and with four different starting structures. Errors indicate the maximum deviation in values observed in any calculation.
[b] 1OMP (Sharff et al., 1992b), apo form of MBP; 1DMB (Sharff et al., 1993), β-cyclodextrin-loaded form of MBP; 1ANF (Quiocho et al., 1997), maltose-loaded complex of MBP; 4MBP (Quiocho et al., 1997), maltotetraose-loaded complex of MBP.
[c] The maximum deviation between any one of the angles calculated by one method versus the average is always 2° or less. The twist angle is ill-defined by the diffusion data (see text).

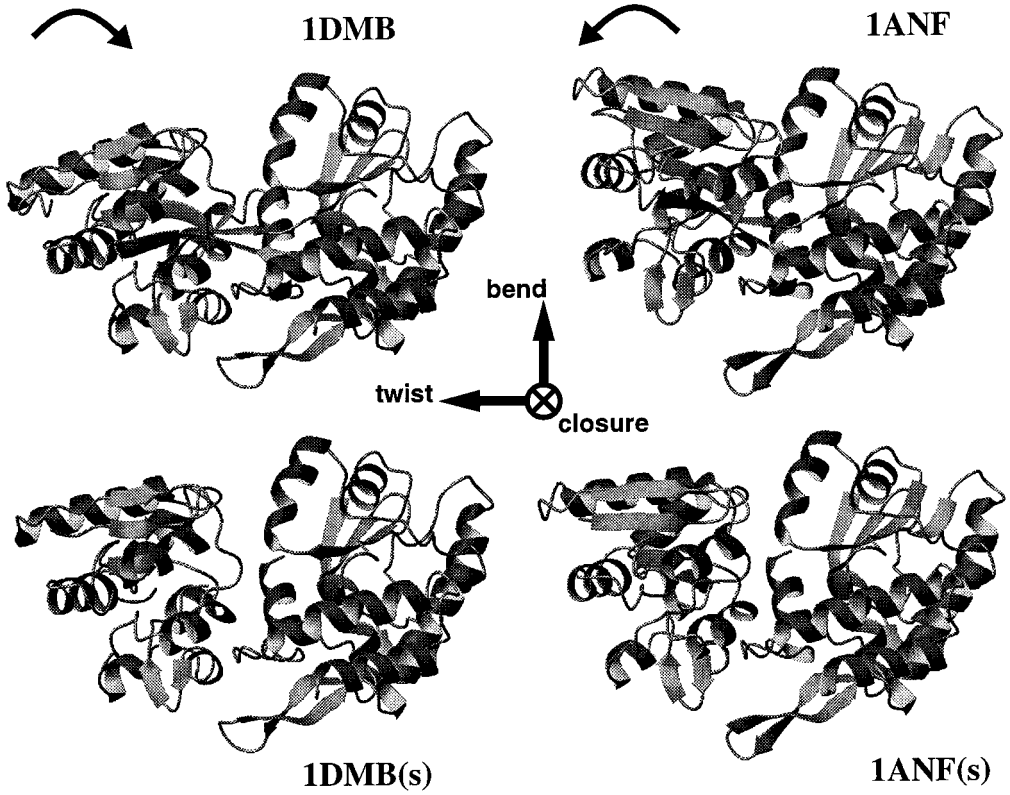

Figure 3. Structures of β-cyclodextrin (1DMB, Sharff et al., 1993) and maltose-bound (1ANF, Quiocho et al., 1997) forms of MBP and the corresponding solution structures, 1DMB(s) and 1ANF(s), obtained by applying rigid body rotations to the N-terminal domains of the parent X-ray structures, as described in the text. The rotations required to transform the X-ray to solution structures are indicated with arrows above the X-ray structures. Each of the rotation matrices used to generate the solution structures was obtained by calculating the average of the rotation matrices derived from the three data analysis protocols discussed in the text and used to align the unique axes of the diffusion tensors of the N- and C-terminal domains. The closure, bend and twist axes are defined as in Skrynnikov et al. (2000) and indicated in the figure. The linker regions in each of the daughter structures are not included. This figure was prepared using MOLSCRIPT (Kraulis, 1991).

of the protein (Sharff et al., 1993). This emphasizes the importance of solution NMR methods for the study of multi-domain proteins that typically adopt different conformations in response to biological stimuli.

Acknowledgements

This research has been supported by a grant from the Medical Research Council of Canada to L.E.K. P.M.H. acknowledges pre-doctoral support in the form of a scholarship from the Medical Research Council of Canada. N.R.S. is the recipient of a Centennial Postdoctoral Fellowship from the Medical Research Council of Canada. L.E.K. is a foreign investigator of the Howard Hughes Medical Research Institute.

References

Alber, T., Gilbert, W.A., Ponzi, D.R. and Petsko, G.A. (1983) *Ciba Found. Symp.*, **93**, 4–24.

Brüschweiler, R., Liao, X. and Wright, P.E. (1995) *Science*, **268**, 886–889.

Clore, G.M., Starich, M.R. and Gronenborn, A.M. (1998) *J. Am. Chem. Soc.*, **120**, 10571–10572.

Cornilescu, G. and Bax, A. (2000) *J. Am. Chem. Soc.*, **122**, 10143–10154.

Faber, H.R. and Matthews, B.W. (1990) *Nature*, **348**, 263–266.

Farrow, N.A., Muhandiram, R., Singer, A.U., Pascal, S.M., Kay, C.M., Gish, G., Shoelson, S.E., Pawson, T., Forman-Kay, J.D. and Kay, L.E. (1994) *Biochemistry*, **33**, 5984–6003.

Fersht, A. (1985) *Enzyme Structure and Mechanism*, 2nd ed., Freeman & Co., New York, NY.

Fischer, M.W., Losonczi, J.A., Weaver, J.L. and Prestegard, J.H. (1999) *Biochemistry*, **38**, 9013–9022.

Fushman, D., Xu, R. and Cowburn, D. (1999) *Biochemistry*, **38**, 10225–10230.

Goto, N.K., Gardner, K.H., Mueller, G.A., Willis, R.C. and Kay, L.E. (1999) *J. Biomol. NMR*, **13**, 369–374.

Hansen, M.R., Mueller, L. and Pardi, A. (1998) *Nat. Struct. Biol.*, **5**, 1065–1074.

Ishima, R. and Torchia, D.A. (2000) *Nat. Struct. Biol.*, **7**, 740–743.

Karplus, M. and McCammon, J.A. (1983) *Annu. Rev. Biochem.*, **53**, 263–300.

Kay, L.E., Torchia, D.A. and Bax, A. (1989) *Biochemistry*, **28**, 8972–8979.

Koenig, B.W., Hu, J.S., Ottiger, M., Bose, S., Hendler, R.W. and Bax, A. (1999) *J. Am. Chem. Soc.*, **121**, 1385–1386.

Kraulis, P. (1991) *J. Appl. Crystallogr.*, **24**, 946–950.

Lee, L.K., Rance, M., Chazin, W.J. and Palmer, A.G. (1997) *J. Biomol. NMR*, **9**, 287–298.

Lipari, G. and Szabo, A. (1982a) *J. Am. Chem. Soc.* **104**, 4546–4559.

Lipari, G. and Szabo, A. (1982b) *J. Am. Chem. Soc.*, **104**, 4559–4570.

Mowbray, S.L. and Sandgren, M.O. (1998) *J. Struct. Biol.*, **124**, 257–275.

Ojennus, D.D., Mitton-Fry, R.M. and Wuttke, D.S. (1999) *J. Biomol. NMR*, **14**, 175–179.

Pawson, T. (1995) *Nature*, **373**, 573–580.

Peng, J.W. and Wagner, G. (1992) *J. Magn. Reson.*, **98**, 308–332.

Pervushin, K., Riek, R., Wider, G. and Wüthrich, K. (1997) *Proc. Natl. Acad. Sci. USA*, **94**, 12366–12371.

Prestegard, J.H. (1998) *Nat. Struct. Biol. NMR supplement* **5**, 517–522.

Quiocho, F.A., Spurlino, J.C. and Rodseth, L.E. (1997) *Biochemistry*, **31**, 10657–10663.

Sass, J., Cordier, F., Hoffman, A., Rogowski, M., Cousin, A., Omichinski, J.G., Löwen, H. and Grzesiek, S. (1999) *J. Am. Chem. Soc.*, **121**, 2047–2055.

Sharff, A.J., Rodseth, L.E. and Quiocho, F.A. (1993) *Biochemistry*, **32**, 10553–10559.

Sharff, A.J., Rodseth, L.E., Spurlino, J.C. and Quiocho, F.A. (1992a) *Biochemistry*, **31**, 10657–10663.

Sharff, A.J., Rodseth, L.E., Spurlino, J.C. and Quiocho, F.A. (1992b) *Biochemistry*, **31**, 10657–10663.

Skrynnikov, N.R., Goto, N.K., Yang, D., Choy, W.Y., Tolman, J.R., Mueller, G.A. and Kay, L.E. (2000) *J. Mol. Biol.*, **295**, 1265–1273.

Spurlino, J.C., Lu, G.Y. and Quiocho, F.A. (1991) *J. Biol. Chem.*, **266**, 5202–5219.

Tjandra, N. and Bax, A. (1997) *Science*, **278**, 1111–1114.

Tjandra, N., Feller, S.E., Pastor, R.W. and Bax, A. (1995) *J. Am. Chem. Soc.*, **117**, 12562–12566.

Tjandra, N., Omichinski, J.G., Gronenborn, A.M., Clore, G.M. and Bax, A. (1997) *Nat. Struct. Biol.*, **4**, 732–738.

Tsan, P., Hus, J.C., Caffrey, M., Marion, D. and Blackledge, M. (2000) *J. Am. Chem. Soc.*, **122**, 5603–5612.

Wider, G. and Wüthrich, K. (1999) *Curr. Opin. Struct. Biol.*, **9**, 594–601.

Woessner, D.E. (1962) *J. Chem. Phys.*, **37**, 647–654.

Zhang, X.-J., Wozniak, J.A. and Matthews, B.W. (1995) *J. Mol. Biol.*, **250**, 527–552.